Limiting processes for diamond epitaxial alignment on silicon

K.-H. Thürer, M. Schreck, and B. Stritzker
Universität Augsburg, Institut für Physik, D-86135 Augsburg, Germany
(Received 5 January 1998)

For the heteroepitaxial deposition of diamond on silicon using the bias-enhanced nucleation procedure, several different processes contributing to the final misalignment of the layers can be identified: (i) The interface of Si/diamond or Si/SiC and SiC/diamond, respectively. (ii) The growth of individual grains during the biasing process. (iii) The growth competition between differently oriented grains and their coalescence during the growth of thick films. X-ray-diffraction texture studies revealed that the azimuthal alignment is essentially determined by the nucleation step. Oriented nucleation is only possible within a defined time window. Within this time window the azimuthal misalignment shows a characteristic variation depending on the absolute value of the bias voltage. The alignment of the SiC interlayer as measured by synchrotron radiation cannot explain the observed variation. In contrast, texture measurements of thick oriented films after exposure to the bias conditions suggest that the limitation of the process time window for oriented nucleation as well as the variation of misorientation with biasing time can be traced back to the detrimental effect of bias-assisted growth. Based on this mechanism, a model is proposed which allows one (a) to describe the temporal development of the azimuthal misorientation within the process time window, and (b) to estimate the contribution of bias-assisted growth on the misorientation. Finally, some epitaxial diamond films have been deposited on high-quality β-SiC layers. A minimum value of 2.9° for the width of the azimuthal distribution has been found. [S0163-1829(98)04923-6]

I. INTRODUCTION

Introduction of the bias-enhanced nucleation process (BEN) provided a powerful method for *in situ* nucleation in diamond chemical vapor deposition (CVD).[1] The method attracted further attention when highly oriented diamond films were realized on β-SiC(001) (Ref. 2) and Si(100) (Ref. 3) more than four years ago. In order to clarify the mechanisms for the BEN process, numerous experimental methods have been used [Raman spectroscopy, Fourier transform infrared spectroscopy, x-ray photoemission spectroscopy,[4,5] and transmission electron microscopy (TEM) (Refs. 6–8)]. Most of the studies concentrated on the pure *in situ* nucleation without consideration of the epitaxy aspect.

With respect to heteroepitaxy, different modifications have been tried to improve the alignment, e.g., precarburization of the substrate,[9] use of the AC bias,[10] and deposition on thin β-SiC layers prepared in a separate CVD process.[11] The latter resulted in films with a polar misorientation of 0.6°. Furthermore, a large number of studies have been performed to characterize the texture and especially the interface of heteroepitaxial diamond films on Si.

Evaluation of the nucleation mechanisms and systematic studies toward an optimization of the epitaxial alignment are hampered by (a) the variety of the interfacial structures found in TEM, (b) the complexity of the processes occurring during the nucleation step, and (c) the difficulty in evaluating quantitative texture data which allow a correlation with the nucleation process parameters. In Fig. 1, the most important phenomena which have been identified experimentally are represented schematically.

Item 1 shows diamond grains in direct contact with the silicon substrate as it has been found by high-resolution TEM.[12] This suggests that a direct nucleation of diamond on silicon may be possible. However, in the same study, diamond grains with a β-SiC interlayer and amorphous carbon as well as oxide have also been observed at the interface. In other studies, the diamond grains were always found on top of a β-SiC interlayer which developed during the biasing step. As shown in item 2, the quality of the two interfaces of Si/SiC and SiC/diamond as well as the crystalline quality of the SiC layer will then contribute to the final (mis)alignment of the diamond grains. The samples characterized by TEM contain mostly interfaces which had developed after the real nucleation event (i.e., during lateral growth of the grains). Since the SiC layer and the carbon phases may change during the duration of the nucleation procedure (typically 10–30 min), and during the subsequent growth, these TEM results have to be discussed very carefully with respect to the role of the different phases for the oriented nucleation. Thus the meaning of the SiC interlayer for the oriented nucleation is still open.

Item 3 shows the growth of diamond grains during the biasing step. First indications that slight misorientation may

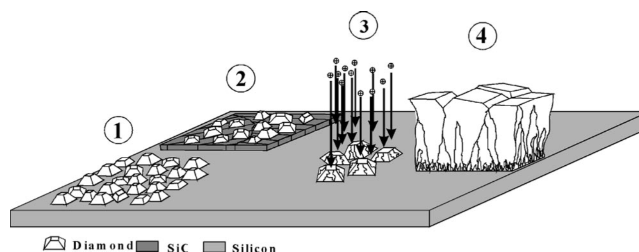

FIG. 1. Phenomena experimentally found in diamond films heteroepitaxially nucleated on Si(001) substrates. (a) Diamond grains in direct contact with silicon without a SiC interlayer. (2) Diamond grains on top of a thin epitaxial β-SiC interlayer. (3) The growth of the diamond grains under bias conditions. (4) Growth competition between and coalescence of individual diamond grains modifying the texture with increasing film thickness.

 © 1998 The American Physical Society

develop during homoepitaxial growth of individual grains under biasing conditions have been reported in Ref. 13. Changes in the growth mode on individual facets have been further studied by scanning electron microscopy (SEM) and TEM.[14] Bias-enhanced nucleation experiments on silicon suggest that bias-assisted growth limits the time for oriented nucleation, and in addition may significantly contribute to the misorientation measured by x-ray diffraction (XRD).[15,16] However, its contribution could not be separated from nucleation effects up to now.

After the nucleation step even the growth without bias modifies the initial texture of the films (item 4). When the wrong growth conditions are chosen, the epitaxy is rapidly lost, favored by the twinning tendency of diamond.[17] The appropriate growth conditions depend on the orientation of the substrate (⟨100⟩- or ⟨111⟩-textured growth). A first simple geometrical model describing this texture development is based on the growth competition between differently oriented grains.[18,19] However, in contrast to pure fiber textures, additional effects may contribute to the texture development in epitaxially nucleated films,[20] e.g., the coalescence of grains with slightly different orientations has been proposed as a mechanism which could help to improve the film texture.[21]

XRD texture measurements always require a certain film thickness, which means that the initial orientation has already been modified. Monitoring the development of the polar and azimuthal components of the misorientation with film thickness revealed that the first could easily be improved by appropriate growth conditions, while the latter was only weakly dependent on film thickness, thus reflecting the misalignment introduced during the nucleation step.[22] From this observation we deduced the concept to quantify the influence of the nucleation process on the misalignment by restricting the evaluation on the pure in-plane component.

In this paper we present experiments which aim at a separation of the different effects described above, and try to quantify their contributions to the final misalignment. It is organized as follows: After a description of the experimental arrangements in Sec. II, the results of texture measurements on diamond films nucleated on Si(001) using the BEN process are presented in Sec. III A. In Sec. III B, the results from synchrotron radiation measurements on the structure of the SiC interlayer are discussed. In Sec. III C, experiments with bias-assisted growth are described. Based on these results, a simulation is presented in Sec. III D which describes the temporal development of the azimuthal misorientation within the process time window for oriented nucleation. Finally, epitaxial diamond films deposited on high-quality β-SiC layers are shown in Sec. III E.

II. EXPERIMENTS

A. Bias-enhanced nucleation on Si(001)

The diamond films were prepared in a microwave plasma chemical vapor deposition (MPCVD) setup as described in Ref. 23. The substrates were mounted on an inductively heated graphite holder. The substrate temperature was measured by a pyrometer. The process conditions are summarized in Table I. During the BEN process, a negative dc bias voltage was applied between the plasma and the substrate holder via a biasing electrode, as described in Ref. 23. After the BEN procedure, the films were grown to similar thicknesses ($\approx$10 μm) in a ⟨100⟩-textured growth process.

TABLE I. Parameters for bias-enhanced nucleation and the subsequent growth step.

	Bias step	Textured growth step
Bias voltage (V)	-180 to -300	-
Process time	15 s–30 min	1200 min
Temperature (°C)	790	790
Microwave power (W)	1300	1300
Pressure (mbar)	45	45
Gas flow rate H_2 (sccm)	180	180
Gas flow rate CH_4 (sccm)	17.5, 1.8	15
Gas flow rate CO_2 (sccm)	0	2.5

In order to quantify the contribution of the SiC interlayer to the misorientation of the diamond films, several samples have been prepared where the whole process was interrupted at different stages of the nucleation step ($U_{\mathrm{Bias}}=-200$ V, substrate temperature 790 °C, 180-sccm H_2 and 17.5-sccm CH_4, and pressure 45 mbar). The structure of these films has been analyzed using synchrotron radiation.

B. Bias-assisted growth experiments

The influence of bias-assisted growth on the texture was studied by applying the biasing conditions typical for the oriented nucleation on Si (substrate temperature of 790 °C, 180-sccm H_2, and 17.5-sccm CH_4) to $\approx$10-μm-thick heteroepitaxially oriented diamond films. The bias exposure time was varied between 20 and 7000 s using bias voltages between -50 and -200 V. The bias step was then followed by a textured growth step (see Table I) for several hours. SEM was then used to decide whether the biasing resulted in a complete loss of epitaxial alignment. A quantitative investigation of the texture modification was performed by x-ray-diffraction measurements of the azimuthal width of the {220} pole density maxima in the plane of the substrate surface, as explained in Sec. II D.

C. Bias-enhanced nucleation on β-SiC

Some deposition experiments have been done using high-quality (001) β-SiC films as substrates. Their misorientation was $<0.2°$ polar and azimuthally. They had been deposited on Si(001) by low-pressure chemical vapor deposition, as described in Ref. 24. The alignment of the diamond films grown on the β-SiC substrates was characterized by azimuthal scans of the {113} β-SiC reflections.

D. Texture measurements

XRD texture measurements on diamond layers with a thickness of several μm were done by a laboratory x-ray diffractometer equipped with an open Eulerian cradle using Cu K_α radiation from a conventional x-ray tube (40 kV, 30 mA). The pure azimuthal misorientation was evaluated directly from the azimuthal width of the {220} pole density distribution at a polar angle $\chi=90°$. This scattering vector lying in the substrate plane is easily accessible in transmis-

sion measurements. The angular resolution for the used configuration was about 1.0°. The transmission measurements required preparation of the samples by etching a 5-mm-diameter hole into the silicon substrates. The ≈10-μm diamond films were easily transmitted by the x rays.

Due to the low thickness of the SiC interlayers formed during BEN on silicon, the bright synchrotron radiation source at the German electron synchrotron DESY was used for their structural characterization. The samples have been analyzed at the HASYLAB beamline B2. Using the translation diffractometer equipped with an Eulerian cradle Θ-2Θ, κ and φ scans were measured. The experiments have been performed at $\lambda=0.154$ nm by using a Si double-crystal monochromator in the primary beam.

III. RESULTS AND DISCUSSION

A. Bias-enhanced nucleation on Si

While *in situ* nucleation by the BEN procedure is easy to accomplish, the oriented nucleation resulting in epitaxial films requires a very careful control of the nucleation conditions. As shown in former work, the duration of the biasing process essentially decides whether epitaxial or purely fiber-textured films are deposited.[16] Figure 2(a) shows the temporal development of the azimuthal distributions of the diamond {220} reflections for a bias voltage of −200 V. The curves can be fitted by Gaussian distributions, with the maximum corresponding to the preferred orientation coinciding with the orientation of the substrate. Below 4 min, a negligible nucleation density was observed, and above 12 min no epitaxy was observed, thus defining a process time window of epitaxial nucleation. Due to the low nucleation density the 4-min sample did not allow sample preparation for the transmission measurements. The values of the full width at half maximum (FWHM) first slightly decrease down to a minimum at 10 min followed by a rapid increase, as shown in Fig. 2(b). Simultaneously the absolute intensities behave contrarily, passing through a maximum. Though the absolute intensities cannot be linearly correlated with nucleation densities of epitaxial grains, they qualitatively reflect the decrease in signal from epitaxial crystallites accompanied by the increase of the fiber texture component. Below 4 min, only a vanishing nucleation density was found. In contrast, above 12 min the films were purely fiber textured though the nucleation density was very high. This latter loss of orientation coincides with the rise in biasing current [see the inset of Fig. 2(a)], resulting from the increasing coverage of the substrate with diamond.

The changes in the film texture for long biasing times indicate two paths for the loss of orientation: a continuous broadening of the orientation distribution, and a rapid complete loss of orientation. Possible mechanisms refer to interface and nucleation or growth phenomena. The first have been studied by characterizing the changes of the β-SiC interlayer at the upper border of the time window. The results will be described in Sec. III B. In addition, experiments on the texture modification by bias-assisted growth will be discussed in Sec. III C.

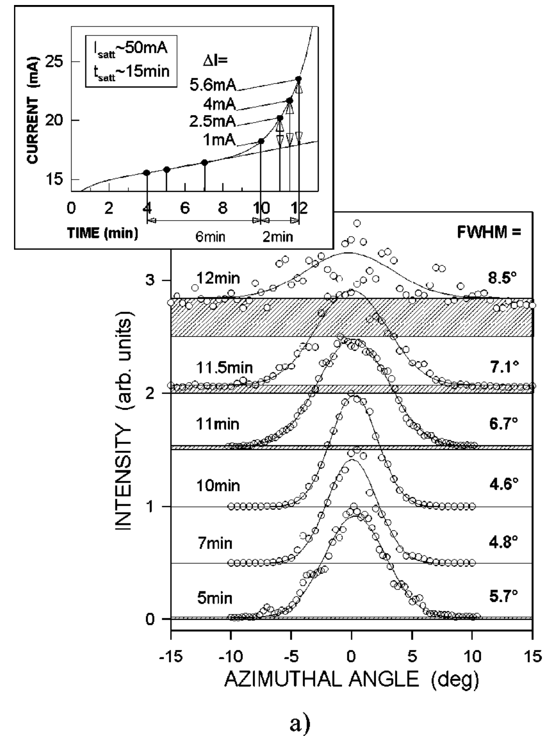

a)

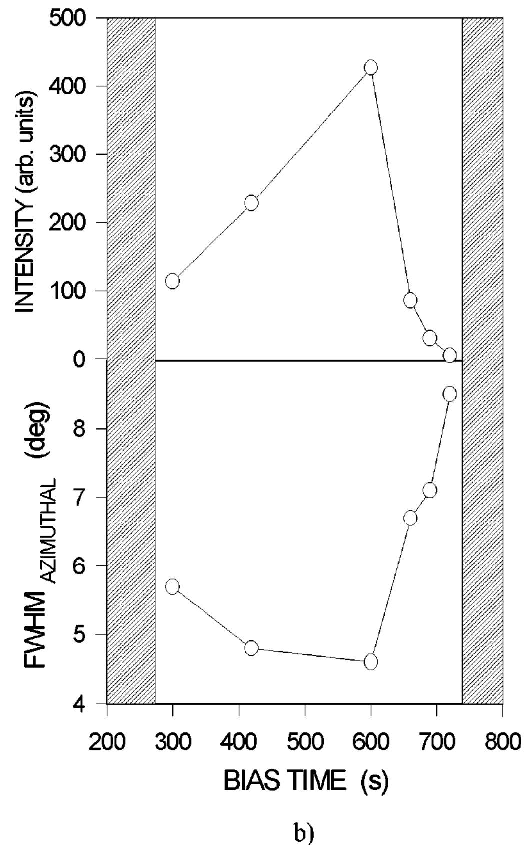

b)

FIG. 2. (a) Azimuthal distributions of the diamond {220} pole densities for films nucleated at $U_{\mathrm{Bias}}=-200$ V varying the duration of the biasing procedure. Hatched areas correspond to the signal from nonepitaxial crystallites. Inset: Temporal development of the biasing current. (b) FWHM's and peak heights of the {220} pole density maxima shown in (a).

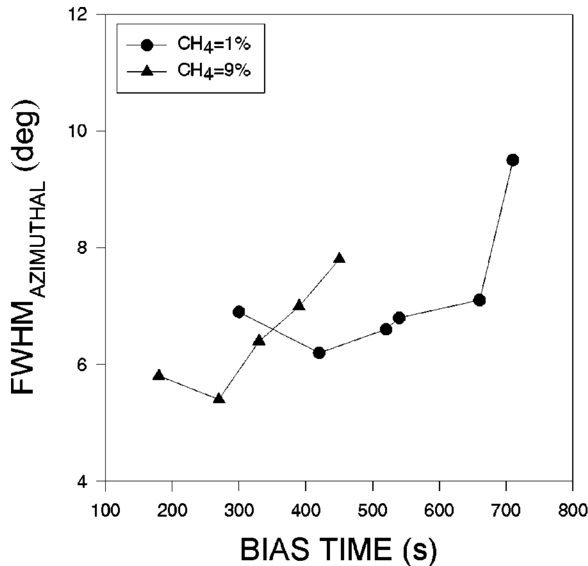

FIG. 3. Full width at half maximum values of the {220} azimuthal pole density distribution vs the biasing time for 1% CH_4 and 9% CH_4 at $U_{Bias} = -210$ V.

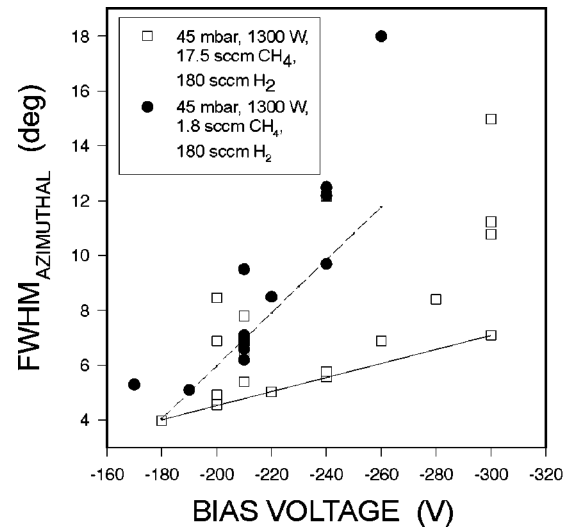

FIG. 4. FWHM of the azimuthal {220} pole density distributions for 1% and 9% CH_4 in H_2 measured for a large number of samples. The straight lines indicate a linear correlation between bias voltage and the minimum values for the azimuthal misorientation.

The results of Fig. 2 demonstrate that evaluation of the influence of a single nucleation process parameter on the epitaxial alignment always requires a scan across this process time window. In order to study the influence of the carbon concentration on the azimuthal misalignment, this procedure has been applied for 1% and 9% CH_4 in H_2. As shown in Fig. 3, the width of the time window for oriented nucleation narrows with the methane concentration. This reflects the accelerated nucleation and growth at higher carbon concentration. With respect to the absolute values for the width of the profiles, deposition at higher carbon concentration yields a slightly better alignment.

From elementary nucleation theory it is known that the deposition rate has a fundamental influence on the film quality.[25] Increasing the methane content results in higher deposition and nucleation rates. This should reduce the available time for the adatoms to reach their equilibrium positions, and also limit the time for clusters to align at the surface. The latter process is especially important when epitaxial alignment is supposed to be a postnucleation phenomenon. In the present experiments higher carbon concentrations in the gas phase did not cause a deterioration in epitaxy. In contrast, they yielded lower values of misalignment. We conclude that the epitaxial quality is not limited by postnucleation rearrangement processes (rotation, migration) of diamond clusters. Similar conclusions have recently been drawn from the observation of a negligible influence of the substrate temperature on the epitaxial alignment.[15]

The bias voltage has a strong influence on the nucleation rate and the alignment.[16] Below some threshold values, nucleation enhancement by the bias voltage is negligible. For the process parameters of Table I in our experimental setup this value is about -150 V. In contrast, at -300 V nucleation densities $>10^9$ cm^{-2} can be achieved within 1 min. The time window for epitaxial nucleation narrows accordingly, showing systematic deterioration in the alignment with increasing biasing time. Evaluating the misorientation within the time window of oriented nucleation for bias voltages between -180 and -300 V, and at CH_4 concentrations of 1% and 9% a map of experimental values as shown in Fig. 4 has been derived.

The minimum value at constant bias voltage and carbon concentration is taken as representative of this set of process parameters. For both gas mixtures a deterioration in the alignment is found with increasing bias voltage. At low carbon concentrations this effect is even more pronounced, thus supporting the conclusion that higher carbon concentrations favor the epitaxial alignment.

B. Structural properties of SiC interlayers formed during BEN on silicon

In former TEM investigations, it has been shown that β-SiC develops under conditions similar to the present one.[7] The predominantly epitaxial β-SiC was very rough with pronounced misorientation, and it changed with biasing time. Epitaxial diamond crystallites with oriented SiC interlayers were found (Fig. 5).

Since TEM can only provide local information, the present synchrotron radiation XRD study was performed (a) to obtain quantitative data about structural properties and the orientation of the β-SiC layer, and (b) to separate its contri-

FIG. 5. High-resolution image of a diamond crystal at the silicon surface. The {111} layers of Si, β-SiC, and diamond (D) are marked (Ref. 7).

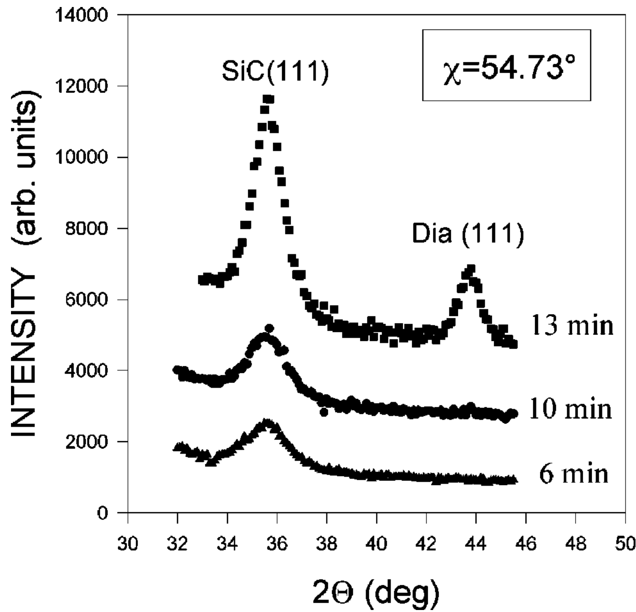

FIG. 6. θ-2θ scans for the SiC(111) reflection measured at the position of the Si(111) reflection (χ=54.73°) for samples biased for 6, 10, and 13 min.

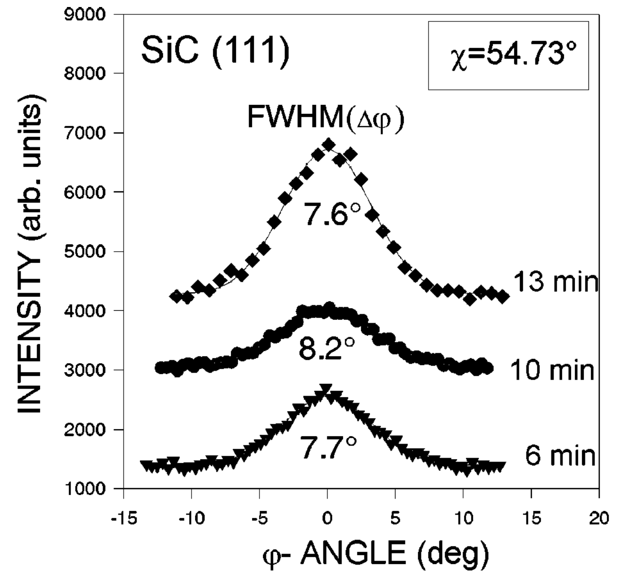

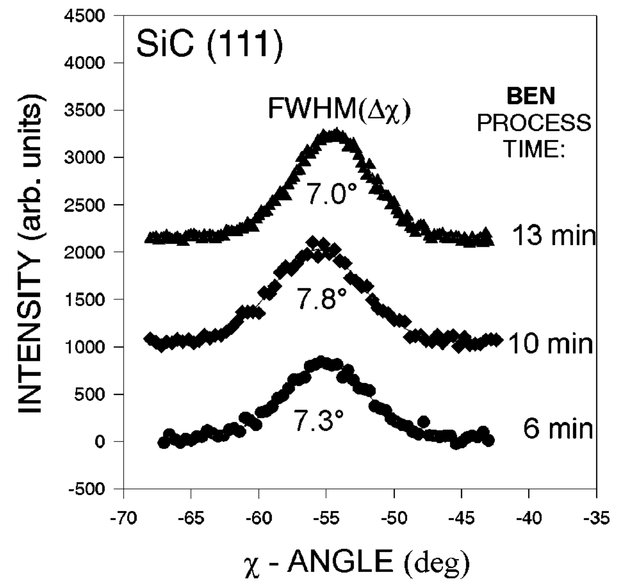

FIG. 7. (a) φ scans and (b) χ scans of the SiC(111) reflection for samples biased for 6, 10, and 13 min.

bution to the misalignment of the diamond layers. Samples were processed for 6, 10, and 13 min under BEN conditions without subsequent growth, corresponding to short, optimal, and delayed nucleation times according to Fig. 2.

Figure 6 shows Θ-2Θ scans of the three samples measured in off-specular direction at a polar angle χ=54.73° corresponding to the orientation of the Si{111} poles. The β-SiC(111) reflections are clearly visible with strongly increasing intensity after 13-min nucleation time. For the longest process time, some signal from diamond was also detectable.

For the further characterization, Θ-2Θ, χ, and φ scans at the specular direction (χ=0°), at χ=54.73° and 72.45° corresponding to the orientation of the substrate reflections (002), (111), and (311), respectively, were measured. Figure 7 shows χ and φ scans for the β-SiC(111) reflections, which confirm the epitaxial alignment with a cube-on-cube orientation relative to the substrate. The data for the FWHM's of all scans are summarized in Table II. Due to the low diffraction intensity the β-SiC(002) profiles for the 6- and 10-min samples could not be evaluated. From the FWHM Δ2Θ, the coherently scattering crystal domain size was deduced using the Scherrer formula.[26] In the last column of Table II, one can see that for all the measured directions the size is between about 4 and 6 nm. According to this nearly isotropic shape, we assume a spherical broadening of the reflections in the reciprocal space for the further analysis of the data.

Two items contribute to the linewidth of the φ and χ scans: the angular spread of the orientation and the crystallite size contribution $\Delta\omega$ with $\Delta\omega = \Delta 2\Theta/(2\sin\Theta)$. According to Ref. 27, the pure orientational component for a scan axis perpendicular to the direction of the reciprocal lattice vector can be deduced by $\sqrt{(\Delta\chi)^2-(\Delta\omega)^2}$ provided that the measured profiles can be described by Gaussian profiles, which applies very well for the present measurements. This size correction (index sc) has been performed for all measured distributions $\Delta\varphi$ and $\Delta\chi$. $\Delta\varphi_{sc}^{**}$ of this analysis for the β-SiC (311) reflections and $\Delta\chi_{sc}^{*}$ for the β-SiC(111) are given in Table II.

As shown in Ref. 22, the broadening $\Delta\chi$ contributes to the width $\Delta\varphi$. Assuming an isotropic tilt, a method has been proposed to deduce the width of the pure azimuthal orientational spread. Applying this analysis to the present data yields $\Delta\varphi_{tsc}^{*}$ and $\Delta\varphi_{tsc}^{**}$ (tsc stands for tilt and size corrected). Both sets of data for the width of the in-plane orientational distribution show a reasonable good agreement.

The present data confirm the formation of epitaxial β-SiC under our BEN conditions on Si(001) substrates. The domain size vertical to the surface as deduced from the linewidth of the Bragg reflections is about 4 nm for the 13-min sample. In a TEM cross-section study of this sample, a β-SiC layer with a varying thickness of up to 7 nm has been observed. The strong limitation of the scattering length parallel to the sur-

TABLE II. Linewidth of the θ-2θ, φ, and χ scans measured at the orientation of the (002), (111), and (311) poles of the Si(001) substrate for three samples with nucleation process times of 6, 10, and 13 min. The procedures for the calculation of the crystal domain size and the FWHM of the $\Delta\chi^{*}_{sc}$, $\Delta\varphi^{**}_{tsc}$, and $\Delta\varphi^{*}_{tsc}$ are described in the text.

SiC(002)						
Nucleation time (min)	$\Delta 2\theta$ (°)	$\Delta\varphi$ (°)	$\Delta\chi$ (°)	-	-	Crystal domain size (Å)
6	-	-	-	-	-	-
10	-	-	-	-	-	-
13	2.6	-	-	-	-	36
SiC(111)						
	$\Delta 2\theta$ (°)	$\Delta\varphi$ (°)	$\Delta\varphi^{*}_{tsc}$ (°)	$\Delta\chi$ (°)	$\Delta\chi^{*}_{sc}$ (°)	Crystal domain size (Å)
6	1.9	7.7	4.5	7.3	6.5	46
10	1.6	8.2	5.6	7.8	7.1	54
13	1.5	7.6	5.2	7.0	6.6	58
SiC(311)						
	$\Delta 2\theta$ (°)	$\Delta\varphi$ (°)	$\Delta\varphi^{**}_{sc}$ (°)	$\Delta\varphi^{**}_{tsc}$ (°)	-	Crystal domain size (Å)
6	2.7	5.9	5.4	5.0	-	38
10	2.5	6.4	6.0	5.5	-	41
13	2.1	5.8	5.5	5.1	-	49

face, which is of the same magnitude as the vertical length, indicates the presence of a high density of crystal defects. The crystal domain size slightly increases between 6 and 13 min. In contrast, the pure azimuthal misorientation, given by $\Delta\varphi^{**}_{tsc}$ and $\Delta\varphi^{*}_{tsc}$, scatters between 4.5° and 5.6° without clear correlation with biasing time.

Our main interest in the structural properties of the β-SiC layer was to clarify its role in the misalignment of the diamond films. As given in Fig. 3, the in-plane orientational spread for the diamond films shows a characteristic variation with process time. Especially at the upper border of the process time window, the distribution broadens rapidly (see also Ref. 16). From the negligible variation of the values in Table II, we conclude that the β-SiC layers do not provide an explanation for the texture modification with biasing time. An alternative explanation is discussed in Sec. III C.

With respect to absolute values, $\Delta\varphi^{**}_{tsc}$ for the β-SiC layers and the width of the azimuthal distributions for the diamond layers prepared under comparable conditions are of the same magnitude. This suggests that for the present process conditions the major fraction of the misorientation arises from the poor quality of the SiC interlayer. On the one hand, the present result motivates the deposition on high-quality β-SiC as the preferable substrate (see Sec. III E). On the other hand, a quantitative deconvolution of the contribution to the misalignment of the diamond film originating from the β-SiC layer would require an ideal layer structure Si/SiC, which provides identical nucleation conditions for diamond over the whole surface. However, lateral inhomogeneities on a sub-μm scale are typically observed by TEM in this work, in accordance with many other TEM studies on the BEN process where SiC of varying crystalline quality and epitaxial alignment, amorphous carbon and even oxide have been reported. Thus the probability for nucleation of oriented diamond depending on all these parameters prevents this evaluation procedure.

Finally, the present values shall be briefly compared with results from synchrotron x-ray diffraction measurements by Je and Noh[28] on the microstructure of the β-SiC layer that developed after ultrasonic treatment of the silicon substrate with diamond powder. The authors found that the ultrasonic treatment with diamond powder strongly enhanced the growth of the SiC layer. Up to 2 h, the thickness of the layer continuously increased, reaching values of 9 nm on Si(100). For the orientational spread (FWHM), values of about 3° for deposition on Si(001) have been reported. As compared to the present study, the thickness of the β-SiC layers is significantly higher, which may be traced back to the process time, longer by one order of magnitude. In addition, the epitaxial alignment is significantly better than for the β-SiC layers of this work. Since a lower CH_4 concentration in our experiments did not yield an improvement, we see the main differences in (a) the biasing procedure which may cause defects due to the ion bombardment, and (b) the duration of the processes. Further systematic studies would be necessary to clarify whether the orientational spread simply improves with the thickness of the β-SiC layer.

C. Texture modification by bias-assisted growth

For the explanation of the rapid broadening of the distributions in Fig. 2 after surpassing the optimal biasing time of

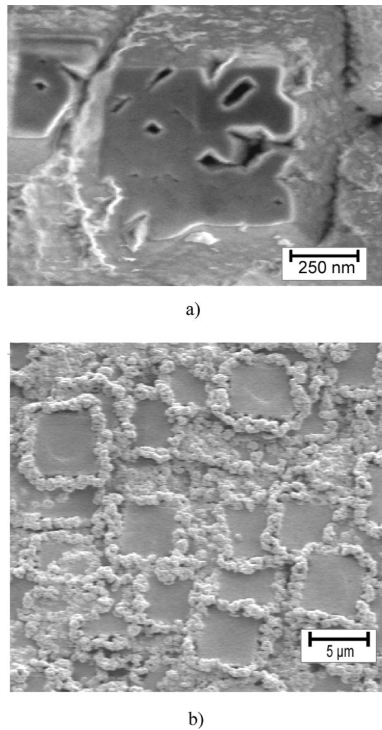

FIG. 8. Scanning electron micrographs of 10-μm-thick diamond films after 15-min exposure to the biasing conditions (see Table I) at (a) $U_{\text{Bias}}=-100$ V and (b) $U_{\text{Bias}}=-200$ V.

10 min and the simultaneous loss of orientation, bias-assisted growth phenomena are one possible explanation. In order to separate the growth phenomena from nucleation phenomena, we applied the biasing conditions to thick ($\approx$10 μm) heteroepitaxially oriented diamond films, and investigated the loss of azimuthal orientation with biasing time and increasing bias voltage.

The morphological changes after 15-min growth under biasing conditions are shown in Fig. 8 for (a) $U_{\text{Bias}}=-100$ V and (b) -200 V. At -100 V, the {100} facets have split into crystalline domains, with the orientation of the underlying diamond grain, which are bordered by [100], [010], and [110], [1-10] edges.[14] At -200 V the centers of the former {001} facets are covered by a flat layer of nanocrystalline diamond, while bulblike structures consisting of amorphous carbon and nanocrystalline diamond grew at their edges.

Whether or not the information about the orientation of the underlying diamond lattice was still transferred during the biasing procedure was deduced from the texture at the film surface after subsequent unbiased growth for several hours under conditions stabilizing a ⟨100⟩ texture. Discrimination between pure fiber textures and partial epitaxial alignment was done by scanning electron microscopy.

Figure 9(a) shows the exposure time necessary for a complete loss of the azimuthal alignment vs the applied bias voltage. At -50 V the epitaxial orientation is preserved even after 5 h of bias treatment. In contrast, at -100 V a pure fiber texture was observed after an exposure time of 60 min. This time interval reduces drastically when further increasing the absolute value of the bias voltage. At -200 V, a 20-s bias treatment suffices to destroy the azimuthal alignment completely.

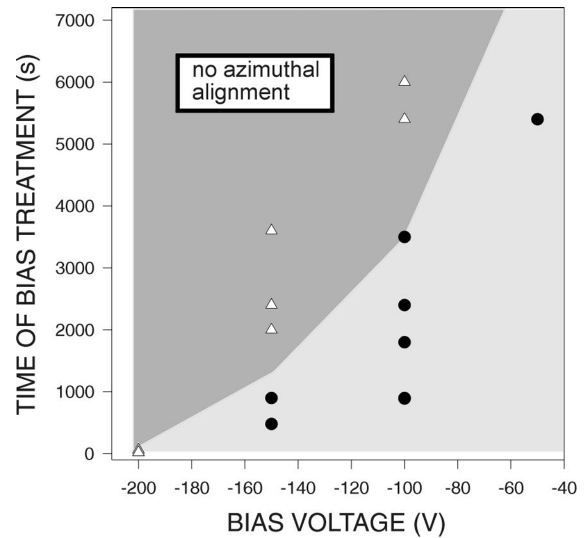

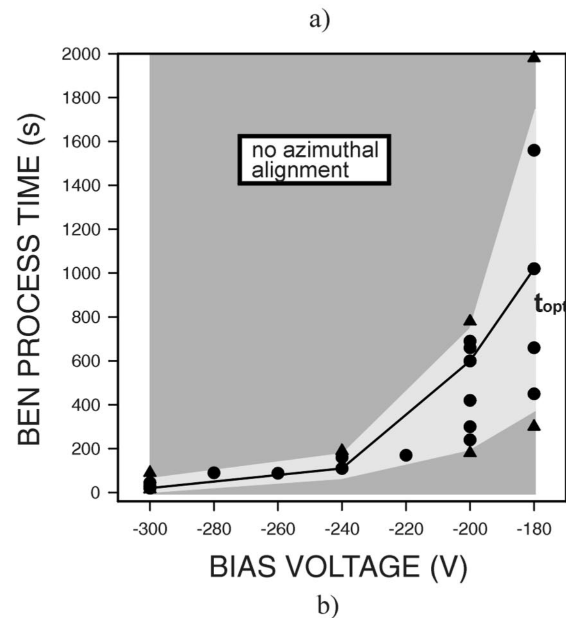

FIG. 9. (a) Exposure time necessary for a complete loss of azimuthal alignment as a function of the applied bias voltage. Filled circles mark films with heteroepitaxial grains present at the surface, while empty triangles correspond to samples for which the azimuthal alignment was completely destroyed by growth under bias conditions. (b) Variation of the process time window for oriented nucleation of diamond on Si(001) with the bias voltage (Ref. 16). Filled circles mark heteroepitaxial films, while empty triangles correspond to samples without preferential azimuthal alignment.

For a direct comparison, the process time window for oriented nucleation of diamond on Si(001) is depicted in Fig. 9(b). This time window narrows from 22 min to 70 s when increasing the bias voltage from -180 to -300 V. Simultaneously, the bias process time t_{opt} for the narrowest azimuthal pole density distributions decreases from about 17 min to 20 s.

Loss of orientation during bias-assisted growth and the limitation of the time window for BEN of heteroepitaxial diamond films on silicon show a similar temporal dynamics. However, they scale differently with the applied bias voltage: While 20 s at -200 V destroys the orientation in Fig. 9(a), the time window at -300 V in Fig. 9(b) amounts to

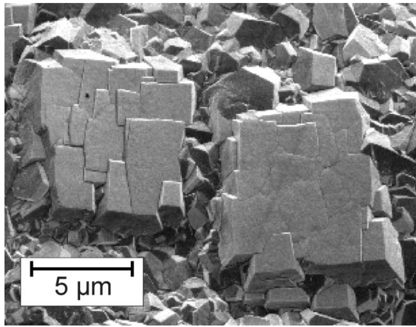

FIG. 10. SEM image of a film after 15-min bias-assisted growth at −150 V and subsequent 6-h ⟨001⟩-textured growth.

about 1 min. This difference results from the enhanced current and electrical field strength above a diamond film as compared to a clean or partially diamond-coated silicon substrate.[16] From the present results we conclude that bias-assisted growth causes the rapid complete loss of the epitaxial alignment at the upper border of the BEN time window.

Figure 10 indicates that the homoepitaxial growth under bias conditions leads to slight misorientations of the single domains relative to the underlying crystallite. In order to study whether these modifications of the local texture result in measurable contributions to the global film texture, and thus may explain the deterioration of the azimuthal orientation for the epitaxial grains observed in Fig. 2, the texture modification caused by bias-assisted growth was determined quantitatively by XRD.

Figures 11(a) and 11(b) show the results for two samples after bias-assisted growth at −150 V for 25 and 45 min, respectively. SEM investigations revealed a pure fiber texture for the 45-min sample, while a preferential in-plane orientation was still visible at the growth surface of the 25-min sample. XRD transmission measurements after removing the silicon substrate showed maxima in the azimuthal profiles for both samples (lower curves in Fig. 11). However, as indicated in Fig. 11(c), the diamond films constitute a system of three layers, i.e., the oriented diamond film which was used as the substrate, the thin layer deposited under biasing conditions, and the upper layer grown at the end under conventional growth conditions. The latter contained the information about the texture modification due to bias-assisted growth. In order to avoid contributions of layers 1 and 2, the samples were successively thinned by bias-assisted plasma etching in a CO_2/H_2 mixture of 2.5:200. The measured azimuthal pole density distributions after different etching times are also shown in Fig. 11. In agreement with the SEM observation the upper layer of the 45-min sample is purely fiber textured. In contrast, the width of the azimuthal distribution for the 25-min sample increases from 7.7° to 11.3°. Taking into account that the first value contains the integral contributions of all three layers, i.e., the alignment of the initial diamond film was better than 7.7°, a broadening due to bias-assisted growth by more than 3.6° can be deduced. The present conclusions are again based on the assumption that the latter growth step without bias does not significantly modify the azimuthal orientation of the epitaxial grains, as has been observed for BEN nucleated layers on silicon.[22]

D. Modeling of the texture modification by growth under biasing conditions during BEN on silicon

According to the results described in Sec. III B, the disturbance of the homoepitaxial growth of diamond grains under biasing conditions can qualitatively explain the broadening of the orientation distribution for long biasing times and the rapid complete loss of orientation which represent two different paths. On the other hand, up to now bias has been of crucial importance in inducing nucleation, and can thus not be avoided. It would therefore be highly interesting to

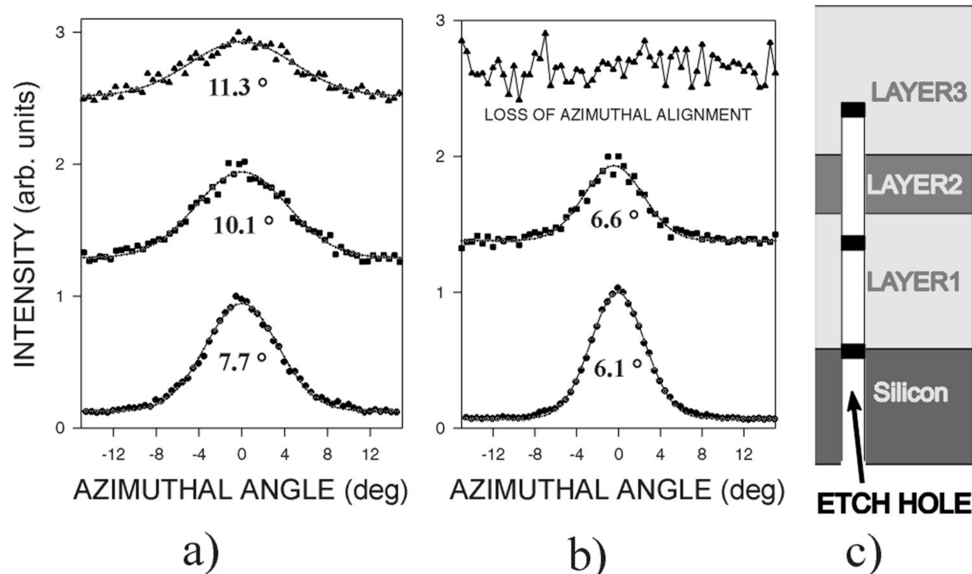

FIG. 11. Azimuthal diamond {220} pole density profiles measured in transmission of epitaxial diamond films after 25-min (a) and 45-min (b) bias-assisted growth at −150 V and a subsequent conventional growth for 10 h. The lower profiles were measured after etching only the silicon substrate. The middle and upper profiles were determined after successively thinning the diamond film. The schematic drawing in (c) indicates the positions of the etching front.

estimate the contribution of this detrimental effect on the measured misorientation under optimum nucleation conditions.

In the following we propose a model which describes the influence of growth under bias on the texture development. The basic elements of this model are the following.

(i) Growth under bias results in a rapid complete loss of orientation. We assume that the probability for this process to occur is constant for every individual grain, independently of its size. Thus the number of oriented grains which populate the substrate surface at a given time t_0 decays exponentially with a characteristic time constant α:

$$g(t-t_0)=\exp[-\alpha(t-t_0)]. \tag{1}$$

Simultaneously the number of epitaxial grains is increased by nucleation processes.

(ii) Bias-assisted growth continuously increases the misalignment for every individual grain by generating defects at the growing surface. The underlying microscopic processes still have to be clarified. Within the present simulation we assume that they are of a statistical character, and each defect can change the orientation by $+\delta\varphi$ or $-\delta\varphi$.

(iii) The pure nucleation process without any modification by bias-assisted growth is already accompanied by a certain (intrinsic) misalignment. An ensemble of diamond grains which have nucleated simultaneously is described by a Gaussian distribution with an initial FWHM of $\Delta\varphi_0$, and a constant r representing the fraction of oriented nucleation events. This distribution broadens by the mechanisms described in Eq. (2). Due to its formal equivalency with a diffusion problem, we use the expression

$$\Delta\varphi(t-t_0)=\Delta\varphi_0\sqrt{D(t-t_0)+1} \tag{2}$$

to describe the temporal development of the width of this distribution.

At time t, the distribution of grains nucleated at t_0 is given by

$$h(t-t_0,\varphi)=r\frac{1}{\Delta\varphi(t-t_0)}\sqrt{\frac{4\ln(2)}{\pi}}\exp\left(\frac{-4\ln(2)}{\Delta\varphi(t-t_0)^2}\varphi^2\right). \tag{3}$$

In this context, D denotes a time constant describing the spreading of the distribution.

Based on the knowledge of the nucleation density $n(t_0)$ and the nucleation rate $\dot{n}(t_0)$, it is possible to simulate the temporal development of the azimuthal distribution as shown in Fig. 2(a) by integrating the product $I(\varphi,t) = r dn(t_0)/dt_0 g(t-t_0)h(t-t_0)$ from $t_0=0$ to t_{BEN}, the duration of the BEN procedure, assuming constant values for $\Delta\varphi_0$ and r during the whole nucleation process. This temporal development was measured by terminating the BEN step after different process times, and then analyzing the samples by SEM. Figure 12 shows a SEM image of a sample after 10 min of BEN at a bias voltage of -200 V.

The data points in Fig. 13 correspond to the nucleation density measured by SEM after different durations of the BEN process at a bias voltage of -200 V. For BEN process times shorter than 5 min, only a very low nucleation density was found, which is usually correlated with an incubation time. Since an additional 60-min growth step did not change the situation, we can exclude that this effect was caused by the limited resolution of our SEM.

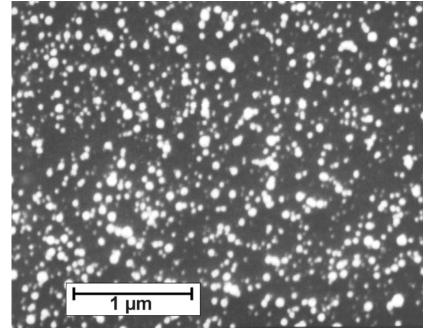

FIG. 12. SEM photograph of a diamond film on Si(001) after 10 min of BEN.

In order to derive an analytical expression for the nucleation rate $\dot{n}$, the measured nucleation densities were fitted by an analytical function which could be differentiated as shown in Fig. 13. The simulation started from the measured initial distribution at 5 min with a FWHM of 5.7°. The $I(\varphi,t)$ dependencies were fitted by varying the free parameters D, α, and $\Delta\varphi_0$ in order to reproduce the experimental result for the temporal development of the misorientation as shown in Fig. 2(b). The result of the simulation for $D = 1.2\ \mathrm{min}^{-1}$, $\alpha=1.4\ \mathrm{min}^{-1}$, and $\varphi_0=3.9°$, and the experimental values, are plotted in Fig. 14 for a direct comparison.

The simulation in Fig. 14 reproduces the experimentally observed minimum. The fit parameter $\alpha=1.4\ \mathrm{min}^{-1}$ corresponds to a half-life period of 0.5 min. The broadening of the distribution given by the simulation for BEN process times >11 min is slower than in the experiment. Additionally, in contrast to the simulation, the experiment indicates a complete loss of orientation for $t>12$ min. Both effects can easily be traced back to the feedback of the growing film on the

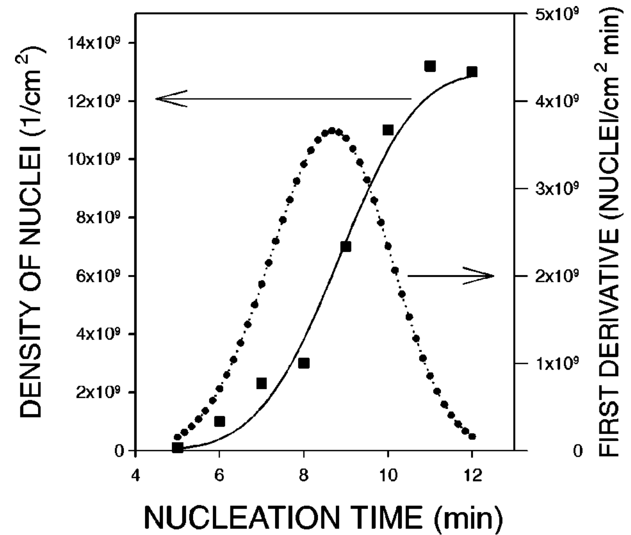

FIG. 13. Nucleation density and the nucleation rate vs BEN process time at $U_{\mathrm{Bias}}=-200$ V.

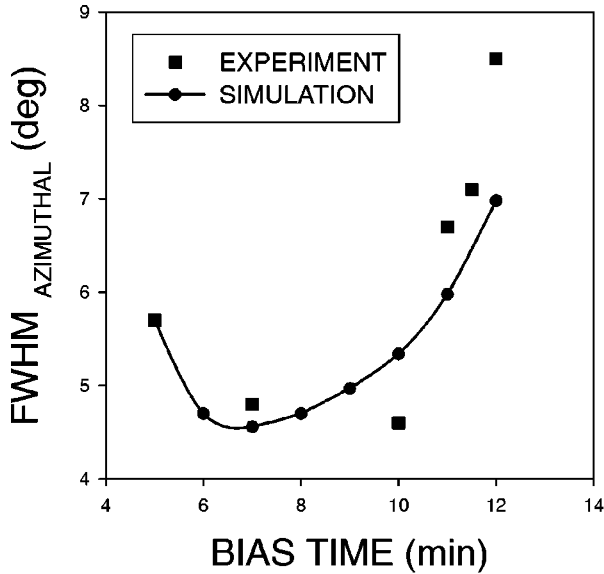

FIG. 14. Experimental values (taken from Fig. 2) for the FWHM of the azimuthal {220} pole density distributions compared with the values deduced from the simulation.

biasing current, and especially the electrical field strength above the diamond-covered substrate, as discussed in Sec. III C. Considering their contribution is beyond the scope of the present simulation.

The most important result of the present simulation refers to the minimum value of $\Delta\varphi$. Comparing the best value of $\Delta\varphi$ (4.6°) with the ''intrinsic'' misorientation $\Delta\varphi_0$ (3.9°) as deduced from the simulation, we conclude that for the termination of the BEN process at the optimum time the contribution of a disturbed homoepitaxial growth due to the biasing conditions amounts to less than 20% of the total misorientation.

E. BEN on high-quality β-SiC layers

In Sec. III B it was shown that the in-plane alignment of the SiC interlayer, which forms under the described experimental conditions during the BEN step, is of rather poor quality. Under the assumption that diamond predominantly nucleates on SiC, the azimuthal alignment of the diamond film is limited by that of the SiC interlayer. Therefore, high-quality SiC layers with angular spreads of in-plane and out-of-plane crystal orientations below 0.2° have been tested as substrates. The BEN process conditions were comparable to those for which the best results on silicon had been obtained.

As compared to silicon, the BEN process was accelerated. Rocking curves for an 8-μm-thick diamond film showed a FWHM of 2.7°. The in-plane component was characterized by φ scans for the {311} reflections, as given in Fig. 15 for the diamond film and the β-SiC substrate. The pure azimuthal component was deduced as described in Sec. III B. For the diamond film the azimuthal misorientation could be reduced to 2.9° as compared to 3.9°, the optimum value realized on silicon up to now.

Despite this improvement there still exists a considerable misorientation. Due to the difficult availability of high-quality β-SiC, systematic parameter studies to find the optimum conditions on β-SiC are still to be done.

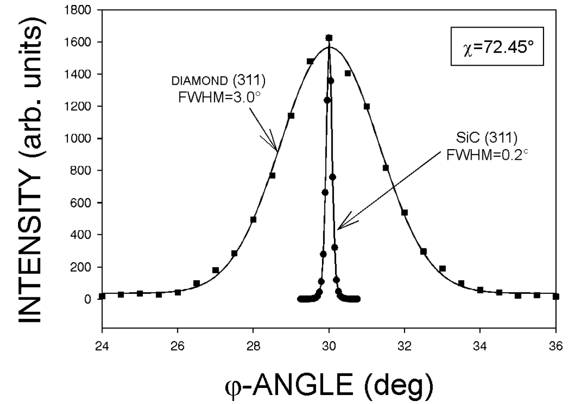

FIG. 15. φ scans for the (311) reflections of diamond and SiC of a diamond/SiC/Si sample.

Investigations by Lannon, Gold, and Stinespring[29] showed that exposure to hydrogen ions modifies a silicon carbide surface and near-surface layers. In surface observations of SiC substrates after negative bias treatment in diamond deposition, pronounced etching has been found.[30] Originally flat β-SiC substrate surfaces exhibited a noticeable stripe morphology immediately after the BEN pretreatment.[31,32] It cannot be excluded that our present BEN conditions change the β-SiC substrate surface negatively, which again deteriorates the epitaxial alignment of diamond. Thus the present result shows the improvement of diamond epitaxy on β-SiC without a decision about its final potential.

IV. SUMMARY

In this work the different processes contributing to the misalignment of diamond films on silicon epitaxially nucleated by the BEN procedure have been studied. Oriented nucleation is only possible within a defined process time window. Restricting to the pure azimuthal spread of the orientation, a characteristic variation with the biasing time has been found. At the upper border of the process time window the distribution broadens rapidly. During the BEN process a thin highly defective β-SiC layer develops. From XRD line broadening, a thickness of about 4 nm was deduced. The absolute value of the orientational spread of this layer is about 5°–6°, indicating that the quality of the epitaxial β-SiC interlayer strongly limits the diamond epitaxy on silicon. Deposition on high-quality β-SiC substrates confirm this result. Due to the high values, a quantitative deconvolution of the interlayer contribution to the diamond misalignment is not possible. We attribute this to the strong lateral inhomogeneities of the interlayer, where areas of different crystalline quality are accompanied by different probabilities for the oriented nucleation of diamond.

According to its negligible variation with bias process time, the alignment of the β-SiC interlayer cannot explain the observed variation of the epitaxial orientation of the diamond films with biasing time. Instead, bias-assisted growth experiments prove a texture modification during homoepitaxial growth of diamond under biasing conditions which can qualitatively explain this behavior.

A simple model was proposed which describes the influence of growth under bias conditions on the texture develop-

ment. The results of computer simulations based on this model are in reasonably good agreement with the experimental data. From the simulation, we conclude that for a termination of the BEN process at the optimum time the contribution of a disturbed homoepitaxial growth due to the biasing conditions amounts to less than 20% of the total misorientation.

ACKNOWLEDGMENTS

The authors would like to thank W. Just from the CS-GmbH Munich for providing the SiC substrates, and gratefully acknowledge financial support by the Deutsche Forschungsgemeinschaft DFG (Contract No. Str 361/4-1) under the auspices of the trinational ''D-A-CH'' Corporation.

[1] S. Yugo, T. Kanai, T. Kimura, and T. Muto, Appl. Phys. Lett. **58**, 1036 (1991).
[2] B. R. Stoner and J. T. Glass, Appl. Phys. Lett. **60**, 698 (1992).
[3] X. Jiang and C.-P. Klages, Diamond Relat. Mater. **2**, 1112 (1993).
[4] W. Kulisch, L. Ackermann, and B. Sobisch, Phys. Status Solidi A **154**, 155 (1996).
[5] M. G. Jubber and D. K. Milne, Phys. Status Solidi A **154**, 185 (1996).
[6] C. J. Chen, L. Chang, T. S. Lin, and F. R. Chen, J. Mater. Res. **10**, 3041 (1995).
[7] P. Wurtzinger, N. Fuchs, P. Pongratz, M. Schreck, R. Heßmer, and B. Stritzker, Diamond Relat. Mater. **6**, 752 (1997).
[8] X. Jiang and C.-P. Klages, Phys. Status Solidi A **154**, 175 (1996).
[9] S. D. Wolter, B. R. Stoner, J. T. Glass, P. J. Ellis, D. S. Buhaenko, C. E. Jenkins, and P. Southworth, Appl. Phys. Lett. **62**, 1215 (1993).
[10] S. D. Wolter, T. H. Borst, A. Vescan, and E. Kohn, Appl. Phys. Lett. **68**, 3558 (1996).
[11] H. Kawarada, C. Wild, N. Herres, R. Locher, P. Koidl, and H. Nagasawa, J. Appl. Phys. **81**, 3490 (1997).
[12] X. Jiang and C. L. Jia, Appl. Phys. Lett. **67**, 1197 (1995).
[13] X. Jiang, W. J. Zhang, M. Paul, and C.-P. Klages, Appl. Phys. Lett. **68**, 1927 (1996).
[14] K.-H. Thürer, M. Schreck, B. Stritzker, N. Fuchs, and P. Pongratz, Diamond Relat. Mater. **6**, 1010 (1997).
[15] M. Schreck, K.-H. Thürer, R. Klarmann, and B. Stritzker, J. Appl. Phys. **81**, 3096 (1997).
[16] M. Schreck, K.-H. Thürer, and B. Stritzker, J. Appl. Phys. **81**, 3092 (1997).
[17] M. Schreck, R. Heßmer, S. Geier, B. Rauschenbach, and B. Stritzker, Diamond Relat. Mater. **3**, 510 (1994).
[18] A. Van der Drift, Philips Res. Rep. **22**, 873 (1967).
[19] C. Wild *et al.*, Diamond Relat. Mater. **2**, 158 (1993).
[20] R. Klarmann, M. Schreck, R. Heßmer, and B. Stritzker, Diamond Relat. Mater. **5**, 266 (1996).
[21] X. Jiang and C. L. Jia, Appl. Phys. Lett. **69**, 3902 (1996).
[22] R. Heßmer, M. Schreck, S. Geier, B. Rauschenbach, and B. Stritzker, Diamond Relat. Mater. **4**, 410 (1995).
[23] M. Schreck and B. Stritzker, Phys. Status Solidi A **154**, 197 (1996).
[24] W. Just, L. Mühlhoff, C. Scholz, and T. Weber, Mater. Sci. Eng., B **11**, 317 (1992).
[25] K. L. Chopra, *Thin Film Phenomena* (Krieger, Malabar, FL, 19XX).
[26] B. D. Cullity, *Elements of X-ray Diffraction* (Addison-Wesley, Reading, MA, 1978).
[27] A. Segmüller, J. Vac. Sci. Technol. A **9**, 2477 (1991).
[28] J. H. Je and D. Y. Noh, J. Appl. Phys. **80**, 2791 (1996).
[29] J. M. Lannon, Jr., J. S. Gold, and C. D. Stinespring, J. Appl. Phys. **77**, 3823 (1995).
[30] T. Yamamoto, T. Maki, and T. Kobayashi, Appl. Surf. Sci. **117/118**, 582 (1997).
[31] N. Marechal and S. Yamashita Jpn. J. Appl. Phys. Part 2 **34**, L1671 (1995).
[32] H. Kawarada, T. Suesada, and H. Nagasawa, Appl. Phys. Lett. **66**, 583 (1995).